ACS APPLIED NANO MATERIALS
Cite This: ACS Appl. Nano Mater. 2018, 1, 5377−5381
Letter
www.acsanm.org

Janus Plasmonic Silver Nanoplatelets for Interface Stabilization

Yichen Guo, Assad U. Khan, Ke Cao, and Guoliang Liu*

Department of Chemistry and Macromolecules Innovation Institute, Virginia Tech, Blacksburg, Virginia 24061, United States

Supporting Information

ABSTRACT: The preparation of Janus plasmonic metal nanoparticles has remained challenging because of their susceptibility to chemical etching and incompatibility with high-temperature processing. Instead of the conventional methods of using Pickering emulsion and vapor deposition, herein Janus silver nanoplatelets (J-AgNPs) with two chemically distinct surfaces are fabricated via a disparate electrostatic adsorption approach. The approach avoids corrosive chemicals and elevated temperatures that degrade the AgNPs. The J-AgNPs show great potential in stabilizing emulsions and forming layered nanostructures at the interfaces. This novel method enables the design of plasmonic nanomaterials at the liquid−liquid and solid−liquid interfaces for colloidal stabilization.

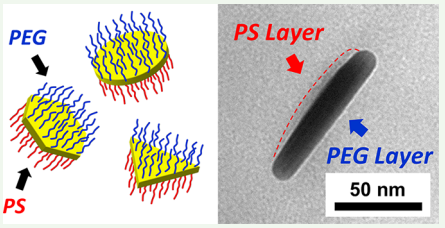

KEYWORDS: *plasmonic, silver nanoplatelets, anisotropic Janus nanoparticles, electrostatic adsorption, interface stabilization*

Janus particles possess two surfaces with distinct physical or chemical properties.[1] Because of their asymmetric properties that isotropic particles lack, Janus particles can effectively stabilize emulsions, self-assemble into ordered structures, and control mass transport at the interfaces,[2,3] and therefore they have found applications in colloidal stabilization,[4] optical/biological sensing,[5] and drug delivery.[6] Most Janus particles studied so far have a spherical shape, and the preparation methods are well-developed for such isotropic shapes.[2] Recently, researchers have explored the preparation of Janus particles with anisotropic shapes such as rods,[7] cages,[8] and platelets (sheets).[9] Among the various shapes, Janus nanoplatelets have a high aspect ratio and a high surface-area-to-volume ratio for molecular adsorption and interaction. The two-dimensional (2D) geometry also restricts their rotation at the interfaces, making them more efficient colloidal interfacial stabilizers than the isotropic spherical counterparts.[10] In general, the fabrication of Janus nanoplatelets is often realized by the following methods: (1) using the Pickering emulsion to mask and functionalize the two sides, respectively;[9] (2) crushing Janus hollow spheres into Janus nanosheets;[11] (3) sequentially functionalizing the exposed sides of the 2D materials from chemical vapor deposition into Janus nanosheets.[12] These techniques are powerful in preparing Janus nanoplatelets such as graphene, graphene oxide, transition-metal dichalcogenides (TMDs), and magnetic metal oxides.[11−14] The preparation of Janus plasmonic metal platelets, however, has remained a challenge because of the incompatibility of the plasmonic metal crystals with these methods.

Plasmonic nanoplatelets made of noble metals such as gold and silver exhibit unique optical and plasmonic properties. The localized surface plasmon resonance (LSPR) of nanoplatelets is tunable across the visible and near-infrared (NIR) ranges, which is difficult for isotropic nanospheres. Owing to the tunable LSPR, plasmonic nanoplatelets are widely used in sensing, imaging, and catalysis.[15−18] Plasmonic nanoplatelets, if they are Janus and are positioned at the interface between two materials, can potentially enable interfacial catalysis and sensing of molecules transporting across the interfaces.[19] Compared to Janus nanospheres[20−23] and 2D graphene, graphene oxide, and TMDs,[11−14] the preparation of Janus plasmonic metal nanoplatelets is extremely challenging because the high-aspect-ratio nanoplatelets are susceptible to chemical etching and thermally induced shape evolution at elevated temperatures.[24]

In this work, we report the preparation of Janus silver nanoplatelets (J-AgNPs) using a method free of corrosive chemicals and high-temperature processing. Using electrostatic attractions, silver nanoplatelets (AgNPs) with negative charges are deposited on glass surfaces, which are coated with positively charged polymers to mask one side of the 2D nanoplatelets. After hydrophilic poly(ethylene glycol) (PEG) is grafted to the exposed side, the resulting PEG-functionalized silver nanoplatelets (AgNPs-PEG) are detached from the glass substrates and further functionalized by hydrophobic polystyrene (PS) on the other side. The resulting J-AgNPs show excellent capability of stabilizing aqueous/organic interfaces and forming interfacial structures on PS beads.

AgNPs were synthesized via a seed-mediated method. The nanoparticles were capped by citrate and had no observable polymers on the surfaces.[25,26] Citrate endowed negative charges to the AgNPs and prevented them from aggregating. In addition, the small citrate molecules minimized impedance to the subsequent grafting of polymer molecules onto the AgNP surfaces.[27] J-AgNPs were fabricated using a facile masking approach coupled with layer-by-layer (LbL) assembly (Scheme 1). First, a glass slide was exposed to oxygen plasma for 10 min to create negative charges on the surfaces. The

Received: July 5, 2018
Accepted: October 11, 2018
Published: October 11, 2018

DOI: 10.1021/acsanm.8b01141
ACS Appl. Nano Mater. 2018, 1, 5377−5381

Scheme 1. Fabrication of J-AgNPs[a]

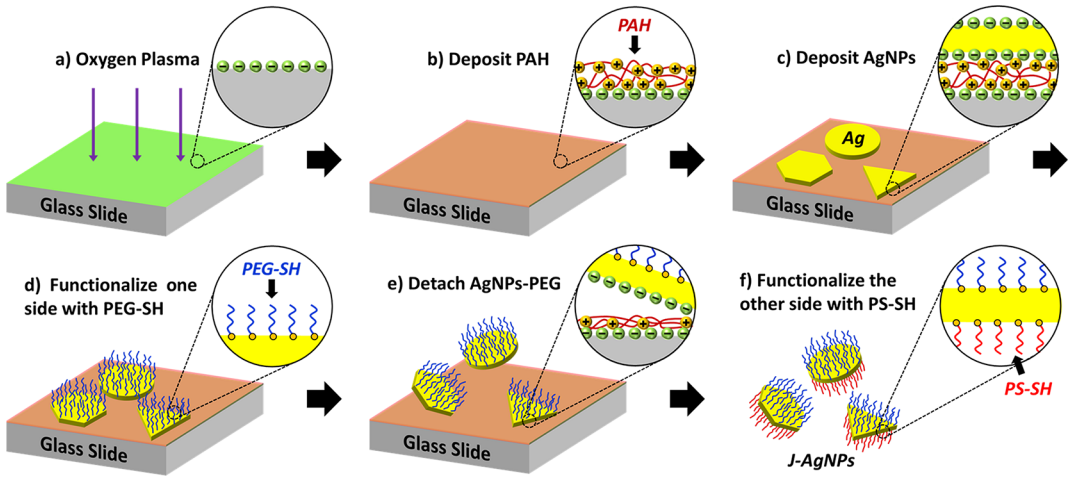

[a](a) A glass slide is treated by oxygen plasma to generate negative charges on the surface. (b) A thin layer of PAH is deposited on the glass via electrostatic attraction. (c) Negatively charged AgNPs including triangles, nanodisks, and hexagons are deposited on the glass, and one side is masked for polymer grafting. (d) The exposed side of the AgNPs is functionalized by PEG-SH. (e) The one-side AgNPs-PEG are detached from the glass via sonication in a NaOH solution (pH = 11). (f) The other side of the AgNPs is functionalized by PS-SH to generate J-AgNPs. Three types of nanoplatelets including triangles, nanodisks, and hexagons are shown for illustrative purposes.

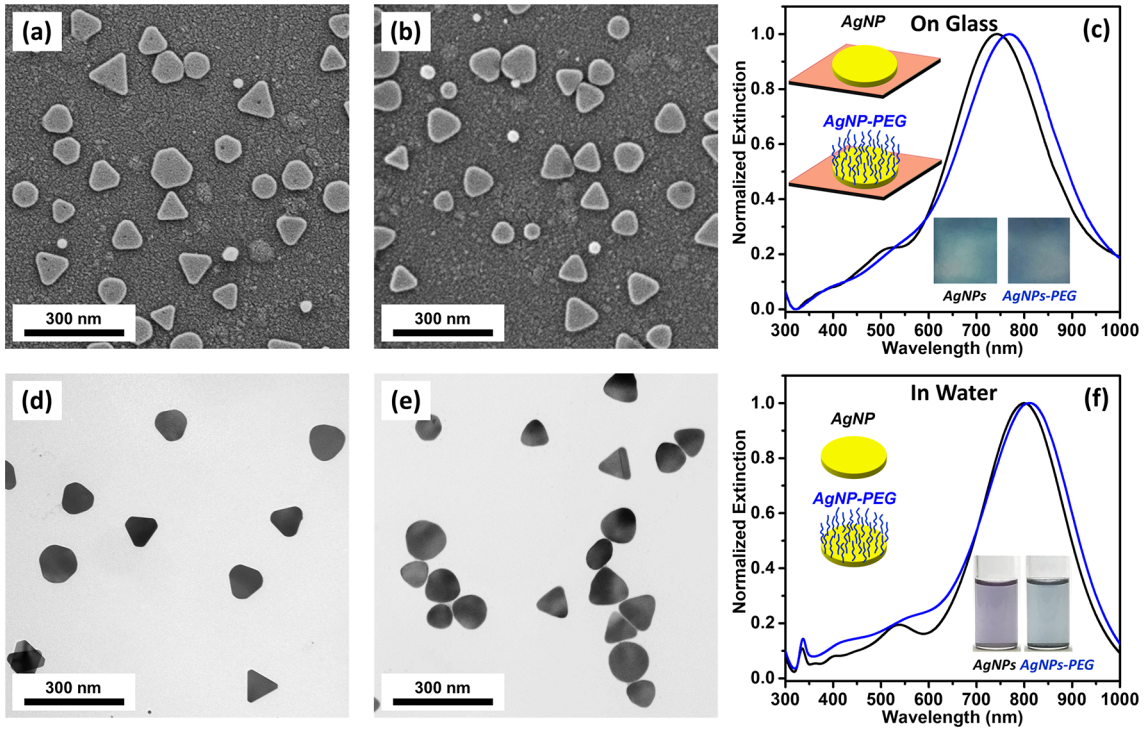

Figure 1. SEM images of (a) AgNPs and (b) AgNPs-PEG on glass slides. (c) Normalized UV−vis−NIR spectra of the AgNPs and the AgNPs-PEG on glass slides. TEM images of (d) AgNPs and (e) AgNPs-PEG. (f) Normalized UV−vis−NIR spectra of the AgNPs and the AgNPs-PEG in water.

negatively charged glass slide enabled the electrostatic deposition of positively charged poly(allylamine hydrochloride) (PAH) to form a thin polymer layer. The PAH thin layer was then used as an active surface for depositing negatively charged AgNPs (Scheme 1a−c). Scanning electron microscopy (SEM) showed AgNPs uniformly adsorbed on the glass slide, with one side being masked by the substrate (Figure 1a). The exposed side of the AgNPs was functionalized by thiolated PEG (PEG-SH) through immersion of the glass slide into an aqueous solution of PEG-SH (0.01 wt %) for 24 h (Scheme 1d). The glass slide was rinsed with deionized water to remove any loose PEG chains on the surface.

SEM images showed indistinguishable changes in the nanoparticle shape before and after functionalization (Figure 1a,b). The AgNPs-PEG were not apparent. To prove the success in grafting PEG to the AgNPs, ultraviolet (UV)−vis−NIR spectrophotometry was employed to detect the changes in the LSPR wavelength (λ_{LSPR}). The λ_{LSPR} value of plasmonic nanoparticles correlates to the refractive index of the surroundings according to the Lorentz−Lorenz equation.[17]

DOI: 10.1021/acsanm.8b01141
ACS Appl. Nano Mater. 2018, 1, 5377−5381

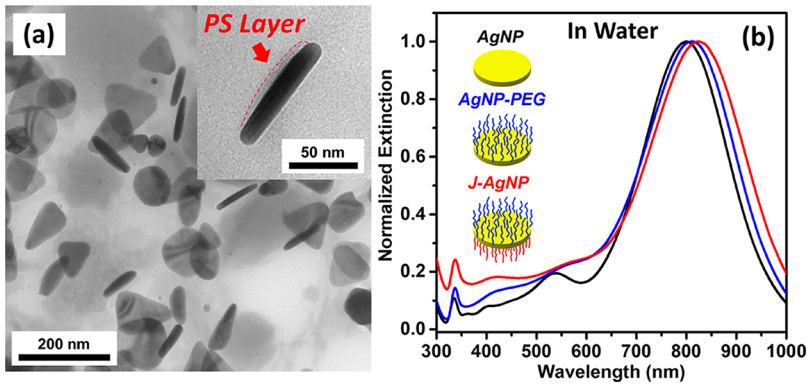

Figure 2. (a) TEM images of J-AgNPs. Inset: Magnified view of a J-AgNP that is vertical to the underlying TEM grid. (b) Normalized UV−vis−NIR spectra of AgNPs, AgNPs-PEG, and J-AgNPs in water.

Compared with the unfunctionalized AgNPs, whose top side was surrounded by air with a refractive index (n) of 1.00, the AgNPs-PEG were covered by PEG with a refractive index of 1.46; therefore, the λ_{LSPR} value of the AgNPs red-shifted from 745 to 770 nm after functionalization with PEG-SH (Figure 1c). The shift of λ_{LSPR} was consistent with the optical graphs of the glass slides (Figure 1c inset), in which the glass slide changed in color from cyan to blue after functionalization. To harvest the AgNPs-PEG, the glass slide was sonicated in sodium hydroxide (NaOH; pH = 11) at 40 °C for 10 min (Scheme 1e and Figure S1). At pH = 11, the ionization degree of PAH decreased to less than 20%,[28] which dramatically weakened the electrostatic attraction between PAH and AgNPs. Hence, the AgNPs-PEG easily escaped from the glass slide upon sonication, allowing for transmission electron microscopy (TEM) characterization (Figure 1e). Compared with the pristine AgNPs (Figure 1d), the shapes of the AgNPs-PEG showed insignificant changes under TEM. The UV−vis−NIR spectra (Figure 1f) show that λ_{LSPR} values of the AgNPs and AgNPs-PEG in aqueous solutions are 800 and 811 nm, respectively. The change in λ_{LSPR} is in agreement with the redshift of λ_{LSPR} on the glass slides. On the basis of the Lorentz−Lorenz relationship, the shift of λ_{LSPR} in water was smaller than that on the glass slide because of the smaller refractive index change from water (n = 1.33) to PEG (n = 1.46) than that from air (n = 1.00) to PEG (n = 1.46) on the one side of the AgNPs.[17]

To functionalize the other side of the AgNPs, the aqueous solution of AgNPs-PEG was centrifuged and then redispersed in *N*,*N*-dimethylformamide (DMF). Afterward, the AgNPs-PEG/DMF solution was mixed with an equal volume of a thiolated PS (PS-SH) solution in chloroform (0.1 wt %). The mixture was constantly stirred for 24 h. Because one side of the AgNPs-PEG was covered by the hydrophilic PEG, the hydrophobic PS-SH can only graft to the other side (Scheme 1f). The resulting J-AgNPs were subjected to 10 cycles of redispersion in chloroform and centrifugation to remove excess PS-SH. TEM (Figure 2a) showed that the J-AgNPs mostly laid parallel to the surface on the TEM grid, and thus it was difficult to identify the Janus structure. The gray areas in the background were probably remaining PS that was not yet completely removed. Some J-AgNPs were almost but not perfectly vertical to the TEM grid, and thus the polymer layer on these nanoparticles cannot be easily observed. Nevertheless, we have identified isolated and perfectly vertically aligned J-AgNPs, as shown in the inset of Figure 2a. One side of the platelet was covered by a faint thin layer. TEM showed that the PEG layer on isotropically PEG-functionalized AgNPs (PEG-AgNPs-PEG) cannot be observed (Figure S2). In contrast, a faint layer was identified on isotropically PS-functionalized AgNPs (PS-AgNPs-PS; Figure S3). Therefore, on the basis of the different visibilities of PEG and PS under TEM, the thin layer observed on the one side of the platelet is ascribed to PS. The thin layer of PS-SH chains was covalently bonded to the AgNP surfaces, as shown in a previous report.[29] If the PS-SH chains were not covalently bonded to the AgNP surfaces, because of the hydrophobic nature of PS and the hydrophilic surfaces of the AgNPs, the PS chains would not form a thin layer but isolated beads on the surfaces to minimize the surface energy. To confirm the surface functionalization, the J-AgNPs were redispersed in water. The UV−vis−NIR spectra (Figure 2b) showed that λ_{LSPR} further redshifted from 811 to 826 nm after functionalizing AgNPs-PEG into J-AgNPs. The size and shape distributions of AgNPs, AgNP-PEG, and J-AgNPs (Figure S4) were similar, indicating that our approach of fabricating Janus particles using electrostatic adsorption had a negligible impact on the size and shape of the AgNPs.

The ability of AgNPs, AgNPs-PEG, and J-AgNPs to stabilize the water/organic solvent interface was tested by mixing the nanoplatelets with water and chloroform mixtures. The three types of nanoplatelets were centrifuged and redispersed in water (2 mL). Afterward, an aliquot of chloroform (30 μL) was added to each solution. Because of their high immiscibilities, water and chloroform phase-separated and the heavier chloroform sank to the bottom of the solution. The mixtures were vigorously vortexed for 1 min to create emulsions. The chloroform phase was agitated into small droplets, which precipitated at the bottom of the solutions. The mixtures were placed on a tilted surface to facilitate the coalescence of chloroform droplets. The coalescence rates of chloroform droplets in the solutions differed drastically. The solution with AgNPs showed the highest coalescence rate, while the solution with J-AgNPs showed the lowest coalescence rate (Figure 3). In the solution with AgNPs, a large droplet of chloroform formed within 5 min. In contrast, the small droplets of chloroform in the solution with J-AgNPs remained well-dispersed. The small droplets of chloroform in the solutions with AgNPs-PEG started to aggregate after 5 min and merged into one single droplet within 24 h. A real-time video (Video S1) visually illustrated that the three types of nanoplatelets had significantly different capabilities of stabilizing the water/chloroform interface. Note that, in the solution with AgNPs-

DOI: 10.1021/acsanm.8b01141
ACS Appl. Nano Mater. 2018, 1, 5377−5381

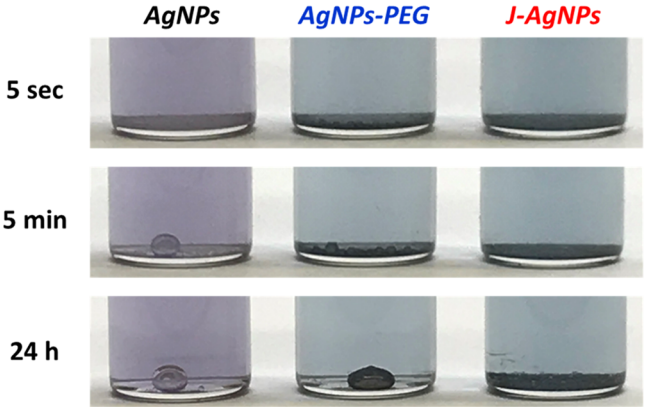

Figure 3. Photographs of the water/chloroform mixtures after the addition of (left) AgNPs, (middle) AgNPs-PEG, and (right) J-AgNPs. The mixtures are vortexed for 1 min and then placed on a tilted surface for (top) 5 s, (middle) 5 min, and (bottom) 24 h to facilitate the coalescence of chloroform droplets.

PEG, the chloroform droplets appeared to be dark blue, indicating that some nanoplatelets were at the water/chloroform interface. Because chloroform is a good solvent for PEG,[30] AgNPs-PEG segregated to the water/chloroform interface, which decreased the interfacial tension and slowed the coalescence of the small chloroform droplets. Similarly, in the solution with J-AgNPs, the small chloroform droplets were blue, indicating that the J-AgNPs also segregated to the water/chloroform interface. Because of the amphiphilic Janus structure, i.e., one side grafted with hydrophilic PEG and the other side with hydrophobic PS, J-AgNPs effectively reduced the interfacial tension between water and chloroform. Consequently, J-AgNPs showed the capability of stabilizing the water/organic interface better than AgNPs and AgNPs-PEG did. Furthermore, compared with the flexible surfactants, the rigid J-AgNPs physically retarded the coalescence at the interfaces.[10] In stark contrast, PS-AgNPs-PS and PEG-AgNPs-PEG were fabricated and subjected to the same emulsion stabilization tests. The results showed that both PS-AgNPs-PS and PEG-AgNPs-PEG were significantly less effective in stabilizing the water/chloroform interface than J-AgNPs (Figure S5).

The J-AgNPs spontaneously formed a layered structure at the interfaces. Aqueous solutions of pristine AgNPs, AgNPs-PEG, and J-AgNPs were mixed with PS latex beads (PSBs) under vigorous agitation. The mixtures were then dropcast onto Si wafers for SEM imaging (Figure 4). None of the hydrophilic AgNPs appeared on the hydrophobic PSB surfaces (Figure 4a). Similarly, the AgNPs-PEG stayed away from the PSB surfaces, and only a few AgNPs-PEG resided in the gap areas (Figure 4b). In stark contrast, a large amount of the J-AgNPs stuck to the PSB surfaces (Figure 4c) and formed a monolayer of nanoplatelets. The morphology can be explained as follows. Upon vigorous agitation, the J-AgNPs were dispersed. The hydrophobic PS-grafted side of the J-AgNPs gradually adhered to the chemically identical PSB surfaces to minimize the interfacial tension.

In summary, we have prepared J-AgNPs with asymmetric surfaces by using electrostatic adsorption to mask, functionalize, and release nanoplatelets. This approach avoids the use of corrosive chemicals or elevated temperatures and thus maintains the integrity of the AgNPs. We have demonstrated that the J-AgNPs can stabilize the water/organic interfaces, prevent emulsion coalescence, and form layered nanostructures on PSBs. The approach of fabricating J-AgNPs using simple electrostatic adsorption presented herein can be extended to the preparation of other Janus plasmonic metal nanoparticles. We envision to prepare nanofilms of Janus plasmonic metal nanoparticles at the solid−liquid and liquid−liquid interfaces, which have great potential in interfacial catalysis, surface-enhanced Raman spectroscopy, and other plasmon-based molecular sensing.

■ ASSOCIATED CONTENT

Supporting Information

The Supporting Information is available free of charge on the ACS Publications website at DOI: 10.1021/acsanm.8b01141.

Description of the experimental materials and methods, UV−vis−NIR spectra, TEM images and size distribution histograms of AgNPs, and optical images of AgNP-coated glass slides (PDF)

Video of water/chloroform mixer stabilization (AVI)

■ AUTHOR INFORMATION

Corresponding Author

*E-mail: gliu1@vt.edu.

ORCID

Yichen Guo: 0000-0002-1637-4440

Assad U. Khan: 0000-0001-6455-3219

Ke Cao: 0000-0001-7204-7455

Guoliang Liu: 0000-0002-6778-0625

Notes

The authors declare no competing financial interest.

■ ACKNOWLEDGMENTS

This material is based on work supported by the National Science Foundation under Grant DMR-1752611. The authors acknowledge the use of facilities within the Nanoscale Characterization and Fabrication Laboratory.

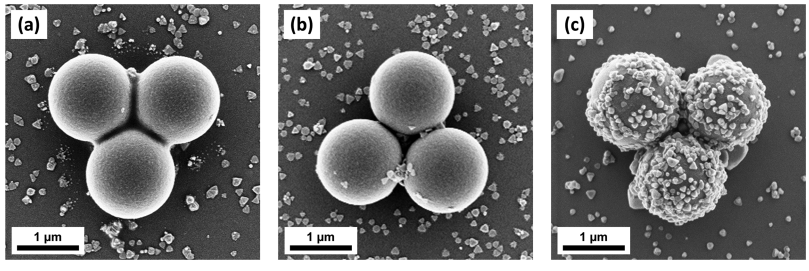

Figure 4. SEM images of (a) AgNPs/PSBs, (b) AgNPs-PEG/PSBs, and (c) J-AgNPs/PSBs mixtures on Si wafers.

DOI: 10.1021/acsanm.8b01141
ACS Appl. Nano Mater. 2018, 1, 5377−5381

REFERENCES

(1) De Gennes, P.-G. Soft Matter. *Rev. Mod. Phys.* **1992**, *64*, 645.
(2) Walther, A.; Müller, A. H. Janus Particles: Synthesis, Self-Assembly, Physical Properties, and Applications. *Chem. Rev.* **2013**, *113*, 5194−5261.
(3) Zhang, J.; Grzybowski, B. A.; Granick, S. Janus Particle Synthesis, Assembly, and Application. *Langmuir* **2017**, *33*, 6964−6977.
(4) Walther, A.; Hoffmann, M.; Müller, A. H. Emulsion Polymerization Using Janus Particles as Stabilizers. *Angew. Chem.* **2008**, *120*, 723−726.
(5) McConnell, M. D.; Kraeutler, M. J.; Yang, S.; Composto, R. J. Patchy and Multiregion Janus Particles with Tunable Optical Properties. *Nano Lett.* **2010**, *10*, 603−609.
(6) Xie, H.; She, Z.-G.; Wang, S.; Sharma, G.; Smith, J. W. One-Step Fabrication of Polymeric Janus Nanoparticles for Drug Delivery. *Langmuir* **2012**, *28*, 4459−4463.
(7) Walther, A.; Drechsler, M.; Rosenfeldt, S.; Harnau, L.; Ballauff, M.; Abetz, V.; Müller, A. H. Self-Assembly of Janus Cylinders into Hierarchical Superstructures. *J. Am. Chem. Soc.* **2009**, *131*, 4720−4728.
(8) Suci, P. A.; Kang, S.; Young, M.; Douglas, T. A Streptavidin−Protein Cage Janus Particle for Polarized Targeting and Modular Functionalization. *J. Am. Chem. Soc.* **2009**, *131*, 9164−9165.
(9) Mejia, A. F.; Diaz, A.; Pullela, S.; Chang, Y.-W.; Simonetty, M.; Carpenter, C.; Batteas, J. D.; Mannan, M. S.; Clearfield, A.; Cheng, Z. Pickering Emulsions Stabilized by Amphiphilic Nano-Sheets. *Soft Matter* **2012**, *8*, 10245−10253.
(10) Xiang, W.; Zhao, S.; Song, X.; Fang, S.; Wang, F.; Zhong, C.; Luo, Z. Amphiphilic Nanosheet Self-Assembly at the Water/Oil Interface: Computer Simulations. *Phys. Chem. Chem. Phys.* **2017**, *19*, 7576−7586.
(11) Liang, F.; Shen, K.; Qu, X.; Zhang, C.; Wang, Q.; Li, J.; Liu, J.; Yang, Z. Inorganic Janus Nanosheets. *Angew. Chem., Int. Ed.* **2011**, *50*, 2379−2382.
(12) Zhang, L.; Yu, J.; Yang, M.; Xie, Q.; Peng, H.; Liu, Z. Janus Graphene from Asymmetric Two-Dimensional Chemistry. *Nat. Commun.* **2013**, *4*, 1443.
(13) de Leon, A. C.; Rodier, B. J.; Luo, Q.; Hemmingsen, C. M.; Wei, P.; Abbasi, K.; Advincula, R.; Pentzer, E. B. Distinct Chemical and Physical Properties of Janus Nanosheets. *ACS Nano* **2017**, *11*, 7485−7493.
(14) Zhang, J.; Jia, S.; Kholmanov, I.; Dong, L.; Er, D.; Chen, W.; Guo, H.; Jin, Z.; Shenoy, V. B.; Shi, L.; Lou, J. Janus Monolayer Transition-Metal Dichalcogenides. *ACS Nano* **2017**, *11*, 8192−8198.
(15) Narayanan, R.; El-Sayed, M. Catalysis with Transition Metal Nanoparticles in Colloidal Solution: Nanoparticle Shape Dependence and Stability. *J. Phys. Chem. B* **2005**, *109*, 12663−12676.
(16) Lee, K.-S.; El-Sayed, M. A. Gold and Silver Nanoparticles in Sensing and Imaging: Sensitivity of Plasmon Response to Size, Shape, and Metal Composition. *J. Phys. Chem. B* **2006**, *110*, 19220−19225.
(17) Willets, K. A.; Van Duyne, R. P. Localized Surface Plasmon Resonance Spectroscopy and Sensing. *Annu. Rev. Phys. Chem.* **2007**, *58*, 267−297.
(18) Khan, A. U.; Scruggs, C.; Hicks, D.; Liu, G. Two-Dimensional Plasmonic Nanoparticle as a Nanoscale Sensor to Probe Polymer Brush Formation. *Anal. Chem.* **2017**, *89*, 7541−7548.
(19) Scanlon, M. l. D.; Smirnov, E.; Stockmann, T. J.; Peljo, P. Gold Nanofilms at Liquid−Liquid Interfaces: An Emerging Platform for Redox Electrocatalysis, Nanoplasmonic Sensors, and Electrovariable Optics. *Chem. Rev.* **2018**, *118*, 3722−3751.
(20) Li, B.; Li, C. Y. Immobilizing Au Nanoparticles with Polymer Single Crystals, Patterning and Asymmetric Functionalization. *J. Am. Chem. Soc.* **2007**, *129*, 12−13.
(21) Song, L.; Qiao, Y.; Liu, Z.; Li, Y. One-Step Synthesis of Janus Hybrid Nanoparticles Using Reverse Atom Transfer Radical Polymerization in Emulsion. *Polym. Chem.* **2015**, *6*, 896−899.
(22) Song, L.; Du, Y.; Teng, C.; Li, Y. Facile Preparation and Self-Aggregate of Amphiphilic Block Nanoparticles. *Colloid Polym. Sci.* **2017**, *295*, 433−439.
(23) Du, Y.; Wei, W.; Zhang, X.; Li, Y. Tuning Metamaterials Nanostructure of Janus Gold Nanoparticle Film for Surface-Enhanced Raman Scattering. *J. Phys. Chem. C* **2018**, *122*, 7997−8002.
(24) Guler, U.; Shalaev, V. M.; Boltasseva, A. Nanoparticle Plasmonics: Going Practical with Transition Metal Nitrides. *Mater. Today* **2015**, *18*, 227−237.
(25) Khan, A. U.; Zhao, S.; Liu, G. Key Parameter Controlling the Sensitivity of Plasmonic Metal Nanoparticles: Aspect Ratio. *J. Phys. Chem. C* **2016**, *120*, 19353−19364.
(26) Khan, A. U.; Zhou, Z.; Krause, J.; Liu, G. Poly (Vinylpyrrolidone)-Free Multistep Synthesis of Silver Nanoplates with Plasmon Resonance in the near Infrared Range. *Small* **2017**, *13*, 1701715.
(27) Hore, M. J.; Ye, X.; Ford, J.; Gao, Y.; Fei, J.; Wu, Q.; Rowan, S. J.; Composto, R. J.; Murray, C. B.; Hammouda, B. Probing the Structure, Composition, and Spatial Distribution of Ligands on Gold Nanorods. *Nano Lett.* **2015**, *15*, 5730−5738.
(28) Choi, J.; Rubner, M. F. Influence of the Degree of Ionization on Weak Polyelectrolyte Multilayer Assembly. *Macromolecules* **2005**, *38*, 116−124.
(29) Choueiri, R. M.; Galati, E.; Thérien-Aubin, H.; Klinkova, A.; Larin, E. M.; Querejeta-Fernández, A.; Han, L.; Xin, H. L.; Gang, O.; Zhulina, E. B.; Rubinstein, M.; Kumacheva, E. Surface Patterning of Nanoparticles with Polymer Patches. *Nature* **2016**, *538*, 79.
(30) Hansen, C. M. *Hansen Solubility Parameters: A User's Handbook*; CRC Press: Boca Raton, FL, 2002.

DOI: 10.1021/acsanm.8b01141
ACS Appl. Nano Mater. 2018, 1, 5377−5381